Effect of Double Interior Stiffeners on the Flexural Behavior of Concrete Filled Steel Tube Composite Box Girders

Hussam Aldin O. Abedi
Civil Engineering Department, Mustansiriayh University, Iraq
Hussamalsodany86@gmail.com (corresponding author)

Mohammed M. Rasheed
Civil Engineering Department, Mustansiriayh University, Iraq
Mmrk72@uomustansiriyah.edu.iq

Received: 19 August 2023 | Revised: 2 October 2023 | Accepted: 5 October 2023

 DOI: https://doi.org/10.48084/etasr.6282

ABSTRACT

A composite box girder is a type of structural element that possesses strong torsional stiffness and resistance against flexural forces. A new category of bridge structure has been established: one that consists of concrete-filled steel tubes connected to composite slabs by steel trusses. In this study, an experimental and computational analysis of flexural loadings on four different types of composite box girders that are connected to concrete-filled steel tubes is presented. The specimens in this test are subjected to a concentrated load at the span's midpoint. The first model is a concrete-filled tube with no internal stiffeners and is used as a control specimen. The second model is a concrete-filled tube with double internal I-shaped stiffeners welded inside a steel tube. The third model features double T-shaped stiffeners, and the fourth model features stiffeners in the shape of a V. When compared with the control specimen, the results of the tests demonstrated that the Concrete-Filled Steel Tube (CFST) section equipped with internal stiffeners provided a better strength capacity and exhibited less deflection. The I- and the V-shaped stiffeners were found to be inferior to the T-shaped. The findings of the numerical analysis were in accordance with the results of the test.

Keywords-composite box girder; concrete filled tube; truss; flexural strength capacity; bridge analysis; finite element; ABAQUS

I. INTRODUCTION

A composite bridge made from steel (girder) and concrete (slab) is the best way to reduce the dead load of the self-weight of the bridge. In recent years, composite bridges constructed with this system contain a top concrete slab with steel trusses and a bottom Concrete-Filled Steel Tube (CFST). This bridge type is limited because it contains a large number of truss joints, so the stress concentration at these joints' location may affect the flexural capacity becomes less [1]. The CFST composite trusses perform duties or services for the load-bearing structural system. The applied moment by the external load is transformed into the axial forces of the upper and lower chords of the truss, while the shear force is turned into the axial force of the webs. The chords in the composite truss are subject to the axial force, so filling the compressive chords with concrete leads to the best solution because of its higher axial strength, and in addition, the concrete core inside the steel tube enhances the buckling behavior of the steel tubes. Also, the steel tube provides more confinement to the concrete core [2]. The experimental results of the composite section under the effect of concentrated load at the mid span of the top slab revealed that the compressive strength of the slab and of the filled steel section (bottom chord), and the steel tube geometry have a significant effect on the strength capacity, crack propagation in the slab, deflection, and slip at the interface between the steel section and concrete, while the shear connectors have a little impact on the load capacity and the deflection and more effect on the slip [3]. According to the concluded remark about the comparison between hollow steel and CFST sections, the CFST section improves the tensile strength by about 11% in comparison with the steel section alone (hollow) [4]. CFST trusses have a concrete-infilled bottom chord and braces for connections. CFST increases the compressive and tensile strength of the chords, which keeps them safe from buckling inward and avoids pinching of the steel tube of the lower chord. It also increases the joint strength and the flexural stiffness of the truss (whole). The hollow steel section reduces the cost because it acts as a formwork for concrete casting [5–8]. Comparison between two trusses, in which the first truss was filled with concrete and the second truss was hollow, was done experimentally and analytically. The strength capacity of the first member was 17.5% higher

than that of the second truss member [9]. Specimens were tested (6 specimens) with different girder trusses to investigate the impact of CFST upper and lower chords of the truss with hollow chords on the welded joints. Based on the test results, the presence of CFST chords increased the load capacity and rigidity of the joint, which prevented chord surface plastic failure [10]. In [11], a total of 8 specimens, i.e. 4 curved, 2 straight CFST, and 2 hollow chord curved truss girders, were tested. The specimens' flexural behavior without the impact of the height/span ratio and the existence of concrete infill was investigated. The stiffness and ultimate load of curved CFST truss girders were found to be higher than that of straight CFST truss girders and curved hollow truss girders [11]. In [12], 4 specimens were tested to explore the effect of the member's layout of truss (diagonal and vertical) connected to the lower and upper CFST members. Different modes of failure appeared, such as surface plasticity, local buckling, shear occurring in the lower chord, and support failure [12]. Authors in [13] investigated the flexural performance of CFST tube truss composites considering different web configurations, such as transverse and transverse braces. The test results showed that the failure mode with diagonal braces was the surface plasticity at the lower or top chord and local buckling. The specimen had diagonal braces and higher load capacity, stiffness, and ductility.

According to the studies mentioned above on the behavior and strength of CFST connected with truss and supported concrete deck slabs, more studies are needed in this research area. The present study focuses on the influence of CFSTs on the flexural performance of composite box girders under static load. The effect of the presence of stiffeners inside of CFST and the influence of the presence of interior stiffeners on the flexural performance of CFST in composite box girders with different shapes such as T, V, and I is investigated in this study. The CFST sections with interior stiffeners had a higher strength capacity and less deflection than the control specimen. The best shape of the stiffeners was the T-shape. The numerical analysis results were in accordance with the test results of [14]. The flexural strength of a concrete girder enhanced by external structural materials due to prior damage was studied in [15]. A bridge may fail due to the action of terrorist attacks such as explosives, so it is needed to make the bridge gliders strong enough [16], something that damages the concrete girders [17]. The use of CFRP laminates significantly affects strand strain, especially with the use of anchors. The CFRP reinforcement affected flexural strength, crack width, and mid-span deflection. However, the flexural stiffness of the strengthened members during the serviceability phases is critical as strand damage ratios increase. In comparison with the non-damaged girder, the NSM-CFRP laminates enhanced the flexural capacity by 11% and 7.7%, corresponding to strand damage of 14.3% and 28.6%, respectively [18].

II. EXPERIMENTAL WORK

Four CFST models that support concrete deck slabs are presented in this study. The model specimens included a control specimen and three specimens with different stiffener shapes welded inside the CFST beam, which are listed in Table I. The geometries of all tested specimens, i.e. composite slabs, connected trusses, and CFSTs, are the same except for the shape of the interior stiffness inside the CFST beam. The width of the specimens is 450 mm, the depth is 400 mm, and the total specimen length is 2000 mm, in which the span from center to center between supports is 1800 mm. The thickness of the concrete deck slab is 100 mm. The truss with a 6 mm thickness is connected to the top concrete slab by a plate with a thickness of 8 mm, in which stud shear connectors are welded in. The diameter of the stud shear connector is 12 mm, distributed with a center to center spacing of 100 mm. A steel tube with a thickness of 1.27 mm was used to fabricate the square tube cross-sections with 150 mm outside depth and width. Based on the selected dimensions, the width/thickness ratio is 118.11, so the tube section is a slender section [21]. The steel tubes and the truss are connected by weld connections. The three tested specimens have the same dimensions with the control specimen but differ by the presence of double internal stiffeners with different shapes provided along the full length of the specimen. The steel stiffeners (I, T, and V shaped) were separately fabricated and welded at their designed locations on a flat steel plate, after which the plate was carefully folded by a press machine to achieve the suggested shape of a cold-formed square steel tube. The square-shaped tube was fabricated by folding the flat steel plate into three folded sides. To complete the tube, the remaining face was formed by fully welding a flat steel plate onto the open edges along the already folded plate using a welding machine. The single stiffeners (long span) are welded inside the steel tube, as shown in Figure 1.

TABLE I. SPECIMEN MARKS AND DESCRIPTIONS

Specimen mark	Descriptions	Stiffeners shape
BG	Composite box girder with truss and concrete filled tubular.	NA
BGWI	Composite box girder with truss and concrete filled tubular with single I-shaped stiffeners.	I
BGWDT	Composite box girder with truss and concrete filled tubular with single T-shaped stiffeners.	T
BGWDV	Composite box girder with truss and concrete filled tubular with single V-shaped stiffeners.	V

NA: Not Applicable

Ordinary Portland Cement Type I was used to cast the concrete deck slab and infill steel tube. The mechanical properties of concrete are listed in Table II.

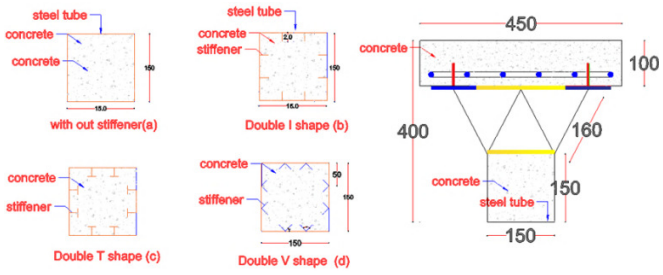

Fig. 1. Specimen details. (a) No stiffeners, (BG), (b) I stiffeners (BGWDI), (c) T stiffeners (BGWDT), and (d) V stiffeners (BGWDV).

The above steel plate is connected with the concrete deck slab by shear connector studs. The geometry and specifications are listed in Tables III and IV, respectively. The concrete deck

slab reinforcement has 10 mm nominal diameter, and spans 100 mm from center to center at both bottom ways (Table V). CFST and steel tube dimensions are listed in Table VI. The mechanical properties of the main reinforcement of the slab can be seen in Table VII, whereas the truss member properties and dimensions are lists in Table VIII.

TABLE II. MECHANICAL PROPERTIES OF SLAB AND FILLED CONCRETE

Compressive strength f_c'	Modulus of rupture f_r	Splitting tensile strength f_t	Modulus of elasticity E_c	Poisson's ratio ν
30 MPa	3.337 MPa	4.244 Mpa	25743 MPa	0.2

TABLE III. SHEAR STUD CONNECTOR-GEOMETRY

Diameter of shear stud connector	Height of stud	Spacing
10 mm	63.5 mm	100 mm

TABLE IV. MECHANICAL PROPERTIES OF THE SHEAR STUD CONNECTOR

Tensile strength f_y	Modulus of elasticity E_s	Poisson's ratio ν
412 MPa	200000 MPa	0.3

TABLE V. CONCRETE SLAB DETAILS

Slab depth	Slab width	Main reinforcement bottom reinforcement
100 mm	450 mm	Ø10@100 in both directions

TABLE VI. FILLING CONCRETE AND STEEL TUBE DIMENSIONS

Concrete	Steel tube		
Depth	Width	Depth and width-square section	Thickness
150 mm	150 mm	150	1.27

TABLE VII. MECHANICAL PROPERTIES OF THE REINFORCEMENTS

Bar diameter	Tensile strength	Modulus of elasticity	Poisson's ratio
10 mm	487.67 MPa	200000 MPa	0.30

TABLE VIII. TRUSS MEMBER DIMENSIONS

Type	Depth	Width	Thickness
Channel	25.4 mm	50.8 mm	6 mm

Fig. 2. Stud shear connector distribution.

Figure 2 shows the location of the stud shear connector distribution along the deck slab that is welded to the upper steel plate. Figure 3 shows the deck slab reinforcement layout. Figure 4 shows the specimen setup and the location of strain gauges, with two of them located at the shear zone as ST1 and ST2 at each support location at the end, while ST3 is located at the bottom center for each specimen. The central point load for each specimen was applied up to failure, and failure and deflection values were recorded. The concentrated load was applied at the mid-span on the top surface of the deck slab gradually up to failure. Strains and deflections were recorded for each load step and then plotted.

Fig. 3. Main reinforcement of the slab layout.

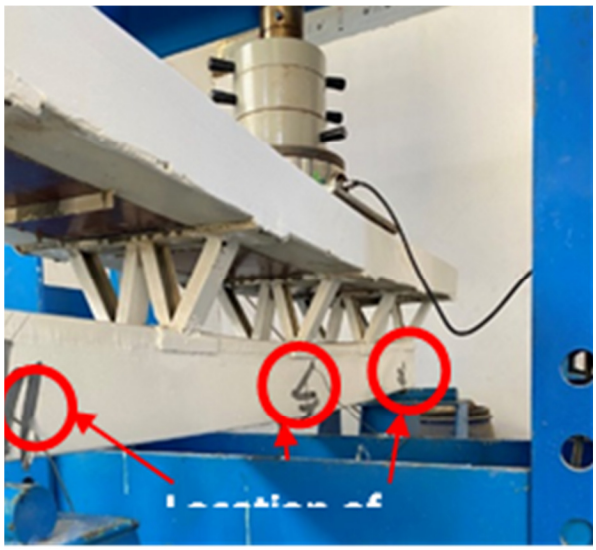

Fig. 4. Location of the strain gauges.

III. TEST RESULTS

In the present investigation, four specimens, including a control composite girder connected by steel truss to CFST without interior stiffeners, and three specimens with stiffeners in I, T, and V shapes were tested under concentrated load. The test results for maximum load capacity, deflection, and strain at maximum load are shown in Table IX. The recorded strain

values listed in Table IX at the locations of ST1 and ST2 are the same but differ when compared with ST3, which is located at the bottom center of the CFST beam. All measured strains had the limited value recommended by ACI-318-2019 [21], which is less than 0.005. Stiffness and ductility of the tested specimens are listed in Table X. Stiffness is calculated by dividing the maximum strength capacity by the corresponding deflection, and ductility, which represents the ability of the structural member to ductile (large deformation) without collapse, is divided by the deflection at failure by the deflection at maximum load capacity. Specimen BGWFDV exhibited the highest stiffness while the lowest was exhibited by the specimen BGWFDI. BGWFDV gave the highest ductility of 1.15 and BGWDI the lowest, equal to 1.09.

TABLE IX. LOAD CAPACITY, MAXIMUM DEFLECTION, AND STRAIN OF THE TESTED SPECIMENS

Model	Load capacity (kN)	Deflection maximum load (mm)	Deflection failure (mm)	Maximum strain $\times 10^{-3}$		
				ST1	ST2	ST3
BG	168.70	15.53	16.88	0.00103	0.00106	0.00071
BGWFDI	206.8	19.5	22.05	0.00096	0.001	0.00017
BGWFDT	234.8	15	18	0.00052	0.00051	0.00033
BGWFDV	251.1	20	23	0.0005	0.00051	0.00031

The behavior and strength of the tested specimens are represented by load deflection and load strain and were recorded for each specimen and each applied load step. Figure 5 shows the load-deflection variations for the tested specimens. In general, the variation started as linear up to the inflection point and the stiffness of the specimen decreased due to the increase in applied load and the increase in deflection. The inflection points for each specimen differ in magnitude due to differences in the connection of unfilled concrete with steel tubes to form the CFST section. Specimen BGWV gave higher strength capacity with lower deflection followed by BGWT, BGWI, and BG.

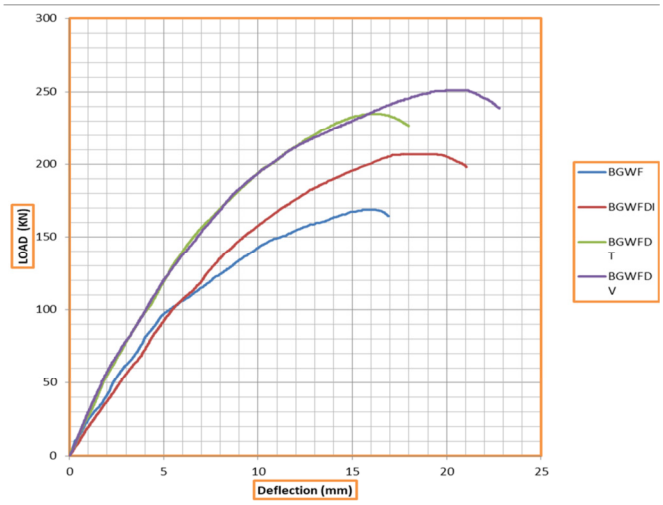

Fig. 5. Load-deflection relation of the tested specimens.

Figures 6-8 represent the load-strain variations of the tested specimens, in which ST1 and ST2 represent the strain at the left and right diagonal tension at supports, and ST3 represents the strain at the middle of the bottom of each specimen. The recorded ST1 and ST2 are almost equal. The strain of the specimen BGWFDV was lower at the supports due to the connection stiffener type, followed by BGWFDI, BGWFDT, and BG. The ST3 of control specimen BG gave a lower strain than the other specimens. The specimens were tested up to failure due to the presence of steel sections that are more ductile than concrete, and the results showed that the presence of interior stiffeners led to a reduction in deflection, an improvement in strength load capacity, and a reduction in strain.

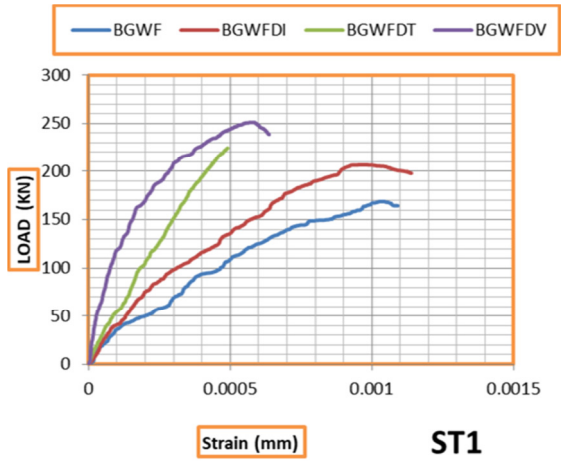

Fig. 6. Load-strain ST1 of the tested specimens.

TABLE X. STIFFNESS AND DUCTILITY OF THE TESTED SPECIMENS

Model	Increase of strength load capacity (%)	Deflection at the load of BG (mm)	Decrease in deflection (%)	Stiffness (kN/mm)	Ductility
BG	---	15.53	---	10.86	1.09
BGWFDI	22.58	11.14	28.26	10.6	1.13
BGWFDT	39.18	7.3	53	15.65	1.2
BGWFDV	48.844	8	48.5	19.1	1.15

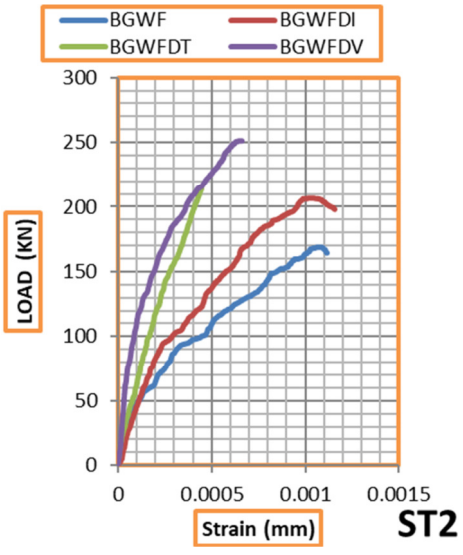

Fig. 7. Load-strain ST2 of the tested specimens.

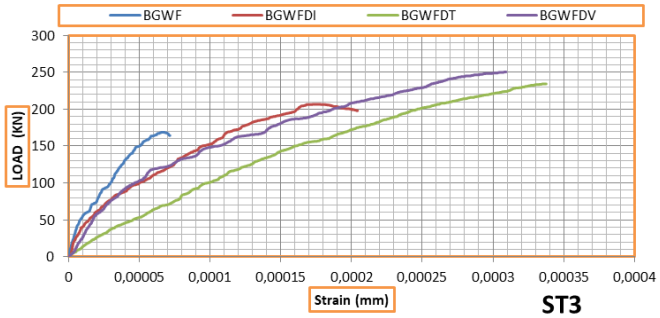

Fig. 8. Load-strain ST3 of the tested specimens.

IV. FINITE ELEMENT ANALYSIS

Finite element models were used to simulate the performance of CFSTs in composite box girders. The concrete element had 8 nodes, the models of the truss elements had 2 nodes, and the steel tube models had 4 nodes. The contact between the concrete and the bottom steel plate, and the concrete and the inner surface of the steel tube involved finite sliding with surface-to-surface formulation, which is the default method in ABAQUS/standard for contact enforcement. A T3D2 with a 2-node linear 3-D truss element was used to simulate reinforcements, stud shear connectors, and stiffeners. The shear stud connector was simulated in such a manner that there was no uplift failure, so it could only deform horizontally due to shear flow. A S4R with 4-node doubly curved shell element was used to simulate the steel tube [21]. Figure 9 shows the finite element model simulation in ABAQUS.

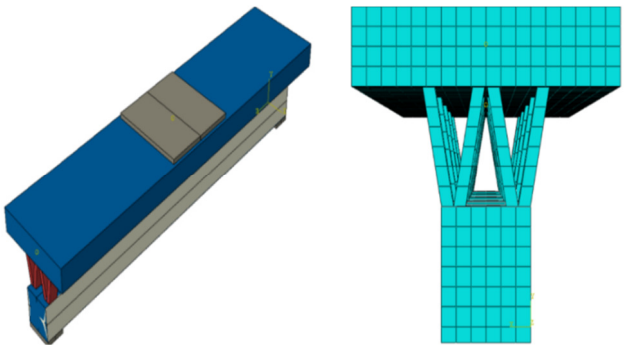

Fig. 9. Finite element model of the whole box girder.

There are two main material modeling approaches for concrete in ABAQUS, which are concrete smeared cracking and Concrete Damaged Plasticity (CDP), which was adopted in the present study. For the CDP model to solve the Drucker-Prager plastic flow function and yield function, five parameters must be defined. Dilation angle, form factor, eccentricity, bi-axial compressive stress ratio, dilation angle, and viscosity. The factors used to model the concrete are listed in Table XI.

TABLE XI. DAMAGE PLASTICITY DATA

Damage plasticity data				
ϕ	e	f_{b0}/f_{c0}	k	ν
31	0.1	1.16	0.667	0

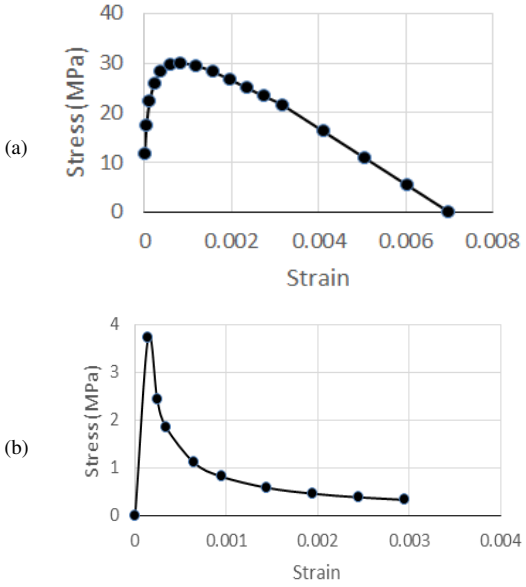

Fig. 10. Stress-strain variation of concrete. (a) Compression, (b) tension.

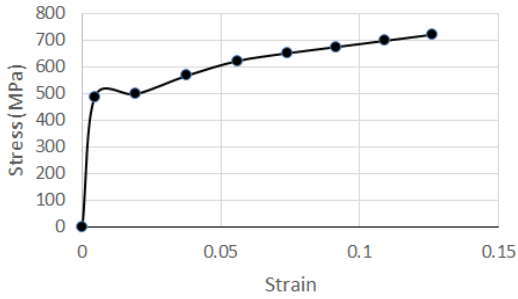

Fig. 11. Stress-strain variation of steel.

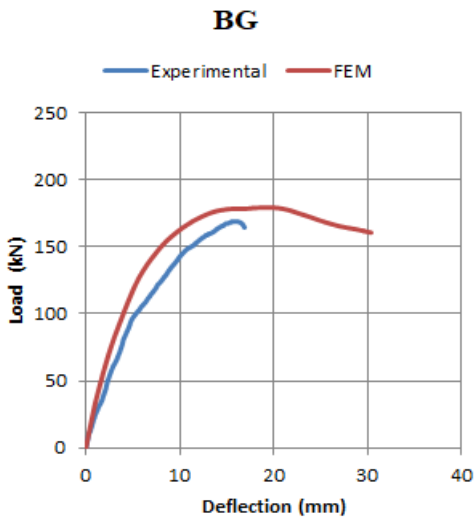

Fig. 12. Experimental and FEM load-deflection relation for the BG specimen.

The stress-strain variation of concrete in compression and tension is presented in Figure 10 while for steel is shown in Figure 11.

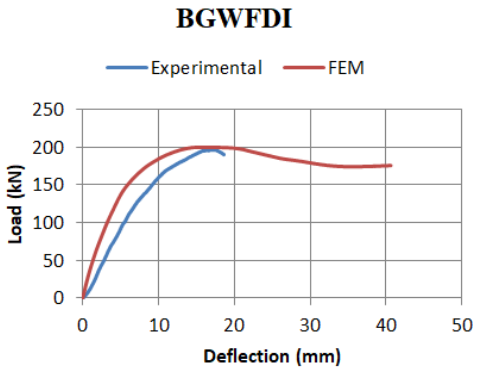

Fig. 13. Experimental and FEM load-deflection relation for the BGWFDI specimen.

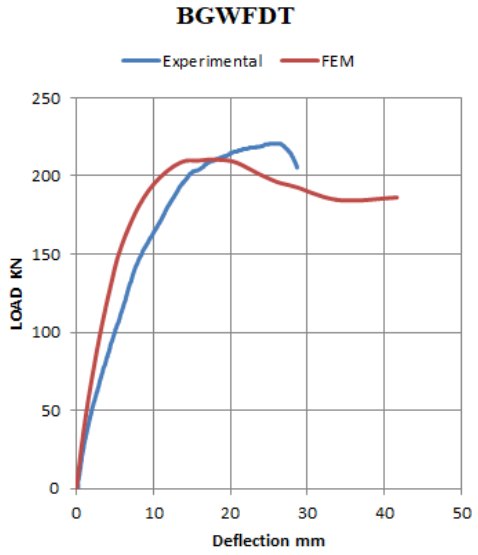

Fig. 14. Experimental and FEM load-deflection relation for the BGWFDT specimen.

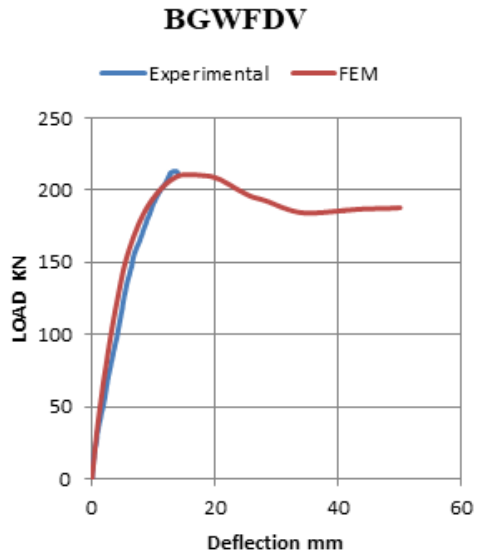

Fig. 15. Experimental and FEM load-deflection relation for the BGWFDV specimen.

Figures 12 to 15 show the load-mid span deflection experimental and FEM results for all specimens. It can be noticed that the results are close. Table XII lists the comparison analysis results. The FEM performance for all simulated models gave lower deflection than the experimental test due to the rigid body of the model and the compatibility between the connected nodes of the elements. Figures 16–19 show the deflection of all models.

TABLE XII. COMPARISON BETWEEN THE EXPERIMENTAL AND THE FEM RESULTS

Model	Load capacity (kN)		Maximu deflection (mm)		FEM/ Experiment	
	Experiment	FEM	Experiment	FEM	Load	Deflection
BG	168.70	179.12	15.53	25.00	1.06	1.06
BGWI	206.8	215.67	19.5	14.75	1.043	0.75
BGWT	234.8	238.43	15	17.55	1.015	1.166
BGWV	251.1	231.50	20	17.22	0.92	0.88

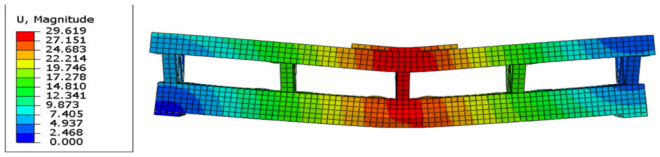

Fig. 16. Deflection of the BG model at failure stage.

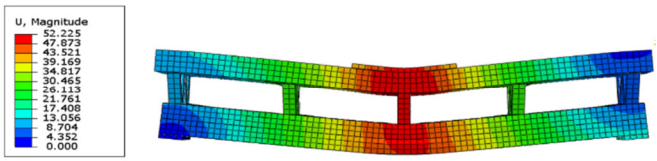

Fig. 17. Deflection of the BGWI model at failure stage.

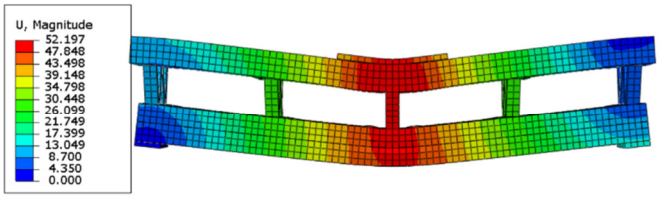

Fig. 18. Deflection of the BGWT model at failure stage.

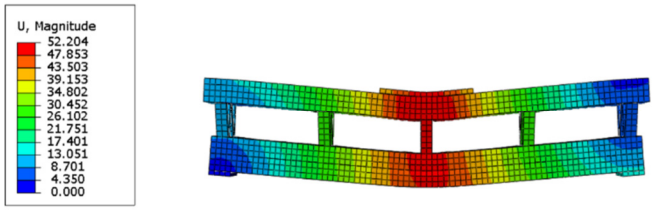

Fig. 19. Deflection of the BGWV model at failure stage.

V. VON MISES STRESSES

The Von Mises stresses are used to check out whether the adopted ductile material will yield or fracture. Figures 20 to 23 show the Von Mises stress distributions for all the simulated models. The stress concentration is at the bottom of the CFST

beam. The minimum stress concentration occurs in the BG model, and the maximum stress occurs in the BGWDI model. The Von Mises stress contours that represent the stress distributions show uniformity. The Von Mises stresses maximum value ranged between 463 and 496 MPa, which means the maximum value is more than the yield strength of the steel tube (383 MPa), so there is a fracture for all models at the failure stage.

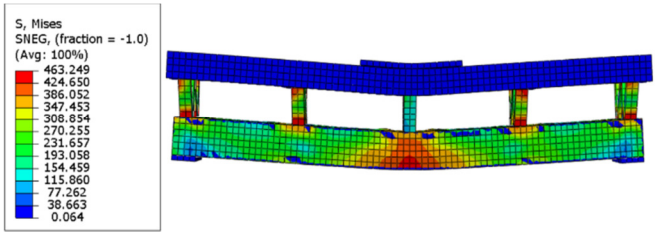

Fig. 20. Von Mises stress of model BG at final loading stage-FEM results.

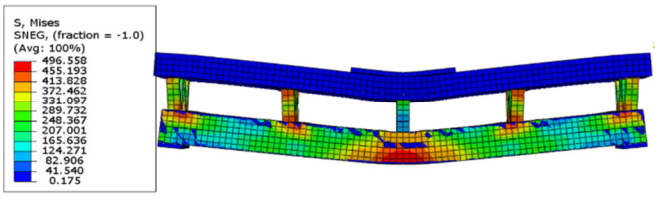

Fig. 21. Von Mises stress of model BGWI at final loading stage-FEM results.

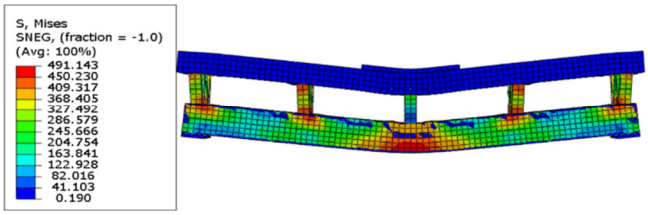

Fig. 22. Von Mises stress of model BGWT at final loading stage-FEM results.

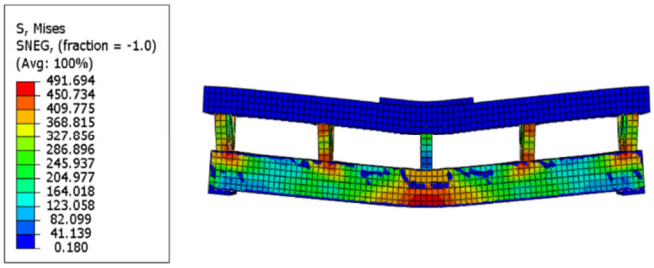

Fig. 23. Von Mises stress of model BGWV at final loading stage-FEM results.

VI. DISCUSSION

The control specimen without interior stiffeners inside the CFST beam had a lower strength capacity because the absence of stiffeners brought a lack of interaction and slip development between the steel tube and the filled concrete. In this case, the resistance force is only the frictional force (adhesive) between the concrete and steel sections. Maximum strength capacity occurs in the presence of T stiffeners because this tube, similar to stud shear connectors, resists the shear flow developed at the interface between filled concrete and steel tube. Specimens with I and V stiffeners had a higher strength capacity than the control specimen, but less than BGWDT. The deflection of specimen BGWDT is less than control's and the specimens with different stiffener shapes because the T section made the composite action more intense and the flange of stiffeners gave a higher resistance to the composite bottom chord. FEM results are close with the experimental results but with less deflection due to the rigid body between the connected nodes of the elements. The number of shear stud connectors designed for full interaction between the steel plate and the deck-reinforced concrete slab that leads to slip at the interface becomes very small or vanishes. No uplift failure occurred between the steel plate and the concrete deck slab during the experiments and in FEM analysis.

VII. CONCLUSIONS

The current work investigated the effect of double interior stiffeners on the flexural behavior of concrete-filled steel tube composite box girders to prevent the slip that may occur at the interface between the filled concrete and the inner face of the hollow steel type and reduce the deflection and stress concentrations along the CFST section by applying double interior studs. This study is an attempt to fill the knowledge gap in this area.

Based on the test and FEM analysis results of four concrete-filled steel tube box girders under flexural load, the following conclusions can be drawn:

- The strength capacity of composite girders connected by truss to the filled steel tube as the bottom chord depends on the presence of interior stiffeners. The presence of interior stiffeners increases the bond between concrete and the interior face of CFST at the interface, which makes the concrete and the hollow steel tube working as one (full interaction) so that there is no slip, therefore the deflection becomes less, the strength capacity becomes higher, and the stress developed as flexural (bending stress) becomes less.
- The strength capacity of composite girders depends on the shape of the stiffeners. The T stiffeners had a stronger capacity than the other types.
- Deflection and strain become less in the presence of stiffeners when compared with the control specimen because there is no slip between the inside concrete and the hollow steel tube.
- The presence of interior stiffeners increases strength capacity and ductility, delaying the occurrence of failure and preventing large deformations.
- The presence of interior stiffeners improves strength capacity due to the increased confinement of hollow steel tubes to the concrete inside. This means that the presence of stiffeners improves the concrete confinement effects.
- FEM results were close to the experimental test results.

REFERENCES

[1] Y. Chen, J. Dong, and T. Xu, "Composite box girder with corrugated steel webs and trusses – A new type of bridge structure," *Engineering Structures*, vol. 166, pp. 354–362, Jul. 2018, https://doi.org/10.1016/j.engstruct.2018.03.047.

[2] Z. Tian, Y. Liu, L. Jiang, W. Zhu, and Y. Ma, "A review on application of composite truss bridges composed of hollow structural section members," *Journal of Traffic and Transportation Engineering (English Edition)*, vol. 6, no. 1, pp. 94–108, Feb. 2019, https://doi.org/10.1016/j.jtte.2018.12.001.

[3] J. R. Joseph and J. H. Henderson, "Concrete–filled steel tube truss girders—a state-of-the-art review," *Journal of Engineering and Applied Science*, vol. 70, no. 1, May 2023, Art. no. 49, https://doi.org/10.1186/s44147-023-00220-w.

[4] L.-H. Han, S.-H. He, and F.-Y. Liao, "Performance and calculations of concrete filled steel tubes (CFST) under axial tension," *Journal of Constructional Steel Research*, vol. 67, no. 11, pp. 1699–1709, Nov. 2011, https://doi.org/10.1016/j.jcsr.2011.04.005.

[5] W. Huang, Z. Lai, B. Chen, Z. Xie, and A. H. Varma, "Concrete-filled steel tube (CFT) truss girders: Experimental tests, analysis, and design," *Engineering Structures*, vol. 156, pp. 118–129, Feb. 2018, https://doi.org/10.1016/j.engstruct.2017.11.026.

[6] Z. Lai and A. H. Varma, "Noncompact and slender circular CFT members: Experimental database, analysis, and design," *Journal of Constructional Steel Research*, vol. 106, pp. 220–233, Mar. 2015, https://doi.org/10.1016/j.jcsr.2014.11.005.

[7] Z. Lai, A. H. Varma, and L. G. Griffis, "Analysis and Design of Noncompact and Slender CFT Beam-Columns," *Journal of Structural Engineering*, vol. 142, no. 1, Jan. 2016, Art. no. 04015097, https://doi.org/10.1061/(ASCE)ST.1943-541X.0001349.

[8] Z. Lai, A. H. Varma, and K. Zhang, "Noncompact and slender rectangular CFT members: Experimental database, analysis, and design," *Journal of Constructional Steel Research*, vol. 101, pp. 455–468, Oct. 2014, https://doi.org/10.1016/j.jcsr.2014.06.004.

[9] S. L. Chqn and M. Fong, "Experimental and Analytical Investigations of Steel and Composite Trusses," *Advanced Steel Construction*, vol. 7, no. 1, pp. 17–26, 2011, http://dx.doi.org/10.18057/IJASC.2011.7.1.2.

[10] W. Huang, L. Fenu, B. Chen, J. Liu, and B. Briseghella, "Resistance of Welded Joints of Concrete-filled Steel Tubular Truss Girders," presented at the Proceedings of the 12th World Conference on Continuing Engineering Education, 2010, https://doi.org/10.3850/978-981-07-2615-7_067.

[11] W. Xu, L.-H. Han, and Z. Tao, "Flexural behaviour of curved concrete filled steel tubular trusses," *Journal of Constructional Steel Research*, vol. 93, pp. 119–134, Feb. 2014, https://doi.org/10.1016/j.jcsr.2013.10.015.

[12] Y. Chen, R. Feng, and S. Gao, "Experimental study of concrete-filled multiplanar circular hollow section tubular trusses," *Thin-Walled Structures*, vol. 94, pp. 199–213, Sep. 2015, https://doi.org/10.1016/j.tws.2015.04.013.

[13] B. Hu and J. Wang, "Experimental investigation and analysis on flexural behavior of CFSTTC beams," *Thin-Walled Structures*, vol. 116, pp. 277–290, Jul. 2017, https://doi.org/10.1016/j.tws.2017.03.024.

[14] H. A. O. Abedi, M. M. Rasheed, and R. A. A. Alwaili, "The Effect of Interior Stiffeners on the Flexural Behavior of Concrete-Filled Steel Tube Composite Box Girders," *Engineering, Technology & Applied Science Research*, vol. 13, no. 4, pp. 11412–11418, Aug. 2023, https://doi.org/10.48084/etasr.6088.

[15] H. Q. Abbas and A. H. Al-Zuhairi, "Flexural Strengthening of Prestressed Girders with Partially Damaged Strands Using Enhancement of Carbon Fiber Laminates by End Sheet Anchorages," *Engineering, Technology & Applied Science Research*, vol. 12, no. 4, pp. 8884–8890, Aug. 2022, https://doi.org/10.48084/etasr.5007.

[16] B. F. Abdulkareem, A. F. Izzet, and N. Oukaili, "Post-Fire Behavior of Non-Prismatic Beams with Multiple Rectangular Openings Monotonically Loaded," *Engineering, Technology & Applied Science Research*, vol. 11, no. 6, pp. 7763–7769, Dec. 2021, https://doi.org/10.48084/etasr.4488.

[17] H. M. Hekmet and A. F. Izzet, "Performance of Segmental Post-Tensioned Concrete Beams Exposed to High Fire Temperature," *Engineering, Technology & Applied Science Research*, vol. 9, no. 4, pp. 4440–4447, Aug. 2019, https://doi.org/10.48084/etasr.2864.

[18] A. J. Daraj and A. H. Al-Zuhairi, "The Combined Strengthening Effect of CFRP Wrapping and NSM CFRP Laminates on the Flexural Behavior of Post-Tensioning Concrete Girders Subjected to Partially Strand Damage," *Engineering, Technology & Applied Science Research*, vol. 12, no. 4, pp. 8856–8863, Aug. 2022, https://doi.org/10.48084/etasr.5008.

[19] *ANSI/AISC 360-16 Specification for Structural Steel Buildings*. AISC, 2016.

[20] ACI Committee 318, *ACI CODE-318-19(22): Building Code Requirements for Structural Concrete and Commentary (Reapproved 2022)*. ACI, 2019.

[21] *Abaqus 6.14 Analysis User's Guide*. Simulia.